

Xichao Sun^{1,2},
Yeqian Ge^{1,*}

Preparation and Properties of Poly(3-hydroxybutyrate-co-3-hydroxyvalerate) and Polypropylene Grafting Maleic Anhydride Two-Component Materials

DOI: 10.5604/01.3001.0011.7298

¹Shaoxing University,
College of Textiles and Garments,
Shaoxing 312000, P. R. China

²Key Laboratory of Clean Dyeing
and Finishing Technology of Zhejiang Province,
Shaoxing, Zhejiang 312000, P. R. China
*E-mail: zhh21080@163.com

Abstract

In order to provide a theoretical basis for the preparation and spinnability of two-component materials, poly(3-hydroxybutyrate-co-3-hydroxyvalerate)(PHBV) and polypropylene grafting maleic anhydride (PP-g-MAH) blends were prepared by melt mixing with different ratios (100/0, 75/25, 50/50, 25/75, 0/100). Properties of the blends system were investigated by means of a mixed rheometer, scanning electron microscope, simultaneous thermal analyzer, differential scanning calorimetry and X-ray diffraction. The results demonstrate that PHBV/PP-g-MAH blends exhibit different morphology of the sea-island with a change in the mix ratio. The initial thermal decomposition temperature of PHBV in the blending system is over 250 °C, which means the thermal stability of PHBV is markedly improved. The crystallisation of PHBV varied according to the blending process parameter. When the cooling velocity increases, the crystallisation peak becomes wide, the temperature of crystallisation decreases, and the crystallisation temperature of PHBV increases significantly. PHBV has a high sensitivity to variation in the shear rate, and PHBV/PP-g-MAH blends have the mixing characteristic of shear thinned liquid. There is no diffraction peak at $2\theta = 22.8^\circ$, and this result certifies that PP-g-MAH changes the crystal form of PHBV. and that PP-g-MAH addition is beneficial to the spinnability of PHBV. Results show that the interplay between PHBV and PP-g-MAH is of great significance and universal for both plastics and fibres.

Key words: PHBV, PP-g-MAH, crystallisation property, thermal property, rheology.

Introduction

In the last decades, synthetic fibres have been progressively developed and have overtaken natural fibres in many fields. However, increasing concern has arisen about their sustainability because of the heavy reliance on non-renewable petroleum resources. The development of bio-based and biodegradable polymers is attracting growing attention as potential substitutes for non-renewable plastics [1-4]. Different types of biodegradable polymers have been studied to produce new polymeric materials with low environmental impacts in recent years [5-9].

Poly(3-hydroxybutyrate-co-3-hydroxyvalerate) (PHBV), as one of the bio-based thermoplastic polymers, is intensively studied due to its potential use in packaging, the automotive industry, biological medicine, and agriculture [10-12]. Nevertheless PHBV has some drawbacks, such as its high crystallisation, brittleness and degradation temperature being close to its melting temperature, which makes it difficult to process [16]. Moreover the market response is far below the expectation, resulting not only from the relatively high price but more from the bottleneck in properties [17]. Therefore it is essential to improve the properties of PHBV with effective methods.

Many efforts [18-20] have been devoted to breaking the above dilemma, including physical blending and block co-polymerisation. Blending PHBV with other polymers such as poly(lactic acid) (PLA), poly(caprolactone) (PCL), poly(ethylene succinate) (PES) and polypropylene(PP) provides interesting routes to control the properties of PHBV. Another potential polymer that can be used to blend with PHBV is polypropylene grafting maleic anhydride (PP-g-MAH). PP-g-MAH is a general-purpose plastic, characterised by stability, high yield, low price, and extensive adaptability. Furthermore it possesses high flexibility, excellent impact strength as well as thermal and chemical resistance [21-22], leading to easy processing. Thus PP-g-MAH is a good candidate for blending with PHBV. As is well-known, blending modification is a common, economical and industrialisation process method [15]. Various researches have concentrated upon the content of the blending component, blending ratio, compatibility between components and not only different processing methods so as to meet the different requirements of new products. However, to the best of our knowledge, study of the preparation of PHBV/PP-g-MAH and its properties is rarely reported.

In this work, a series of PHBV/PP-g-MAH blends were tentatively produced by means of a high-speed mixer and melt-blended in a twin-screw extruder. The structure and phase morphology of the blends were investigated as representations of PP-g-MAH on PHBV. Interestingly the blend showed improved high-crystallisation and heat-resistance, which broke the bottleneck of traditional PHBV. The spinnability was optimised by determining a narrow temperature window for each blend via rheological studies, melt-spinning and hot-drawing, and crystal of the blends was studied by XRD, which indicated that PP-g-MAH addition undoubtedly changed the crystal form of PHBV. The results showed that the interplay between PHBV and PP-g-MAH was of great significance and they can be applied in both plastics and fibres.

Materials

Commercially available PHBV powder and PP-g-MAH chips were used in this work. PHBV powder was provided by Ningbo Tianan Biological Material Co., LTD (China) under the trade name ENMATY, which was additional antioxidants. PP-g-MAH chips (CMPPTM), of which the grafting rate is about 1%, were purchased from Bluestar Co., LTD (China).

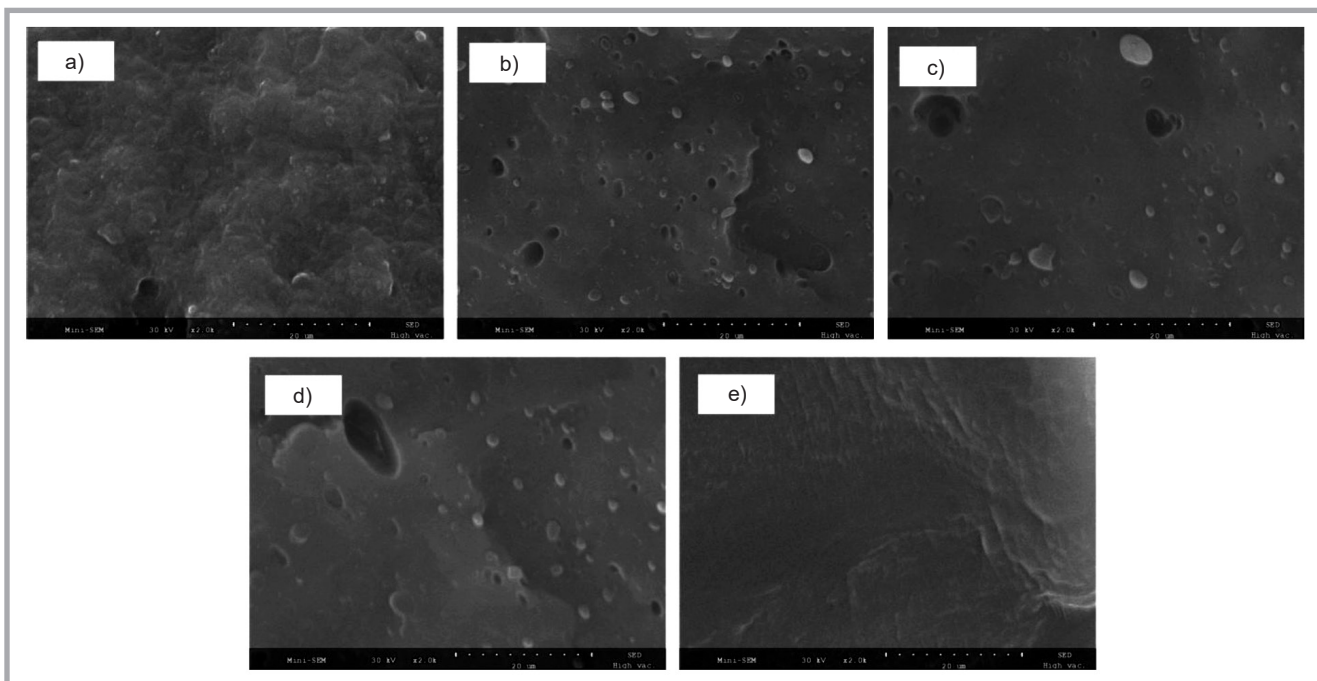


Figure 1. SEM images of PHBV/PP-g-MAH blends with a ratio of PHBV and PP-g-MAH of a) 100:0, b)75:25, c)50:50 d)25:75; & e)0:100.

Preparation of PHBV/PP-g-MAH

PHBV powder and PP-g-MAH chips were dried at 80 °C for 12h in a vacuum oven (Uf260Plus, MEMMERT Company, Germany), then PHBV powder and PP-g-MAH chips were well blended via a high-speed mixer containing 0, 25, 50, 75 and 100wt% PP-g-MAH, and coded as a, b, c, d and e, respectively. The PHBV powder and PP-g-MAH chips were melt-blended in a twin-screw extruder equipped with a gravimetric dosing unit by HAAKE Minilab II hybrid rheometer (Thermo Fisher Scientific Co., LTD., USA).

Scanning electron microscopy

A polymer blend of PHBV/PP-g-MAH was prepared as a dumbbell sample by an injection moulding machine (MiniJet Pro, Netherlands DSM company, Netherlands) at the following conditions: injection temperature 190 °C, injection pressure 700 bar and forming time 10 s. Then the brittle fracture of the samples was induced using liquid nitrogen, and finally the cross section shape of the samples was observed by a SNG3000 scanning electron microscope (South Korea the SEC Co., LTD) after coating with gold.

Thermogravimetric analysis

The thermal stability of various samples was established using thermogravimetric analysis apparatus (TG/DTA6300, Seiko Instruments Inc-SII, Japan). The sample

weight was approximately 7 mg. Experiments were performed in the temperature range 30-650 °C at a heating rate of 20 °C /min in a nitrogen atmosphere. The initial decomposition temperatures were at 10% of the weight loss.

Differential scanning calorimeter

The melting and non-isothermal crystallisation of PHBV/PP-g-MAH blends, PHBV and PP-g-MAH were studied by performing a second heating run in a DSC (DSC-I, Mettler Toledo, Switzerland). The temperature and heat flow were calibrated with indium. Samples of 7 mg were encapsulated in aluminum pans and heated from -10 °C to 210 °C at a heating and cooling rate of 10 °C/min using nitrogen as a purge gas. The thermal history of the samples was erased by preliminary heating (-10 °C to 210 °C range). Measurements were made from the first cooling scan and second heating scan. The temperature then fell to -5 °C at cooling rates of 2 °C/min, 5 °C/min, 10 °C/min, 20 °C/min, and 30 °C/min, respectively. The crystallinity was obtained using the DSC method [14], the formula of which is shown below (1).

$$X_c(\text{PHBV}) = \frac{\Delta H_m(\text{PHBV/PP})}{\Delta H_f(\text{PHBV})} \times \frac{100}{C} \quad (1)$$

Where $\Delta H_m(\text{PHBV/PP})$ (J/g) is the second melting enthalpy of the polymer matrix, $X_c(\text{PHBV})$ the degree of crys-

tallinity of PHBV in the blending system, $\Delta H_f(\text{PHBV})$ the melting enthalpy of pure crystalline PHBV (146.6 J/g) [17], and C is the mass fraction of PHBV in the blending system.

Rheology

The rheological properties of PHBV, PP-g-MAH and their blends were studied at 190 °C using a HAAKE torque rheometer (HAAKE PolyLab QC, Thermo Fisher Scientific Co., LTD., Germany) equipped with a capillary die (D=1.5 mm, L/D=20).

X-Ray diffraction

The crystallisation of PHBV, PP-g-MAH and their blends was studied via a X-ray diffractometer (Empyrean, Netherlands Palmer Naco Co., LTD., Netherlands). Using the Bragg Brentano configuration, 2 θ diffraction diagrams were recorded from 3° to 60° at a rate of 3 °/min.

Melt-spinning and hot-drawing

PHBV, PP-g-MAH and their blends were prepared by means of the HAAKE torque rheometer (HAAKE PolyLab QC, Thermo Fisher Scientific Co., LTD., Germany) equipped with a capillary die (D=0.2 mm, L/D=3). For the purpose of comparison, the winding speed of the winding equipment (Xplore, DSM, Netherlands) was fixed at 25 m/min during drawing, and the total draw ratio was fixed at 1.6, which was the maximum

draw ratio achievable for fibres spun at the highest speed, i.e., 300 m/min.

Results and discussions

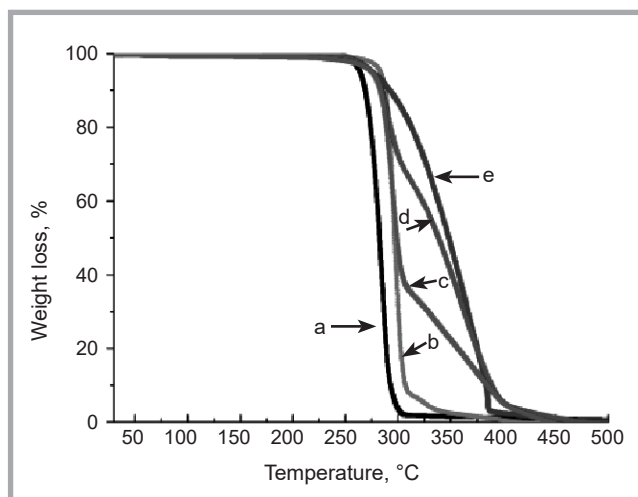
Morphology analysis

The morphology of the PHBV/PP-g-MAH blends (a, b, c, d, e) is presented in **Figure 1**. According to the figure, PHBV and PP-g-MAH are generally an incompatible system, and possess the feature of sea-island distribution. As shown in **Figure 1.a** and **Figure 1.e**, PHBV and PP-g-MAH are a continuous phase. It is seen in **Figure 1.b** that PHBV and PP-g-MAH present a sea-island two-phase dispersion, where PHBV is a sea phase and PP-g-MAH an island phase, and part of PHBV and PP-g-MAH become a continuous phase. According to **Figure 1.c**, the boundaries of two-phase PHBV/PP-g-MAH are unclear, and most of PHBV and PP-g-MAH become a continuous phase. While PHBV and PP-g-MAH appear to be a distinct sea-island two-phase dispersion again, where PP-g-MAH is a sea phase and PHBV an island phase, shown in **Figure 1.d**. That is to say, PHBV and PP-g-MAH are partially compatible. Then the PHBV/PP-g-MAH blends demonstrate different morphology with a change in the composition ratio. When PHBV and PP-g-MAH are at a mass ratio of 50:50, the distribution of PHBV/PP-g-MAH blends are the most compatible.

Thermogravimetric analysis (TGA)

TGA and scans of PHBV, PP-g-MAH and PHBV/PP-g-MAH blends at different ratios are presented in **Figure 2**. Neat materials show one-step decomposition in the nitrogen atmosphere, with the initial thermal decomposition tempera-

Figure 2. TG curve of PHBV/PP-g-MAH blends.



ture (10wt% loss) of neat PHBV being 215°C, and its full thermal decomposition temperature is around 300°C, i.e. the range of the thermal decomposition temperature is 85°C.

The initial thermal decomposition temperature of PP-g-MAH is 60°C higher than for PHBV, whose complete thermal decomposition temperature is around 400°C, and its range of thermal decomposition temperature is about 125°C. It demonstrates that neat PP-g-MAH has better thermal stability.

Compared with neat PHBV, it was found that the initial thermal decomposition temperature of PHBV/PP-g-MAH blends reached over 250°C. The pyrolysis of PHBV/PP-g-MAH blends are mainly divided into three stages, namely the early, middle and late responses in accordance with the moisture evaporation of a single component in the blending system, the fracture of a macromolecular chain caused by thermal decomposition of

PHBV components, and the fracture of the PP-g-MAH component caused by thermal decomposition, respectively. It is likely to be at the beginning of the thermal decomposition reaction of PHBV, with the macromolecular chain of melting PHBV in the center of the local randomly generating some activation [16-17]. While the thermal decomposition mechanism of PP-g-MAH is more complex, mainly showing a macromolecular and ester exchange reaction, which is reversible in molecules and intermolecular. Melting PHBV/PP-g-MAH blends may lead to an ester exchange reaction. On one hand, this reaction inhibits the generation of an activation center in PHBV, thus enhancing the thermal stability of PHBV. On the other hand, it promotes the pyrolysis of PP-g-MAH, consequently reducing the thermal decomposition temperature of the PP-g-MAH, which is consistent with literature [14]. In summary, PP-g-MAH blending can increase the thermal stability of PHBV and further broaden the processing window of PHBV.

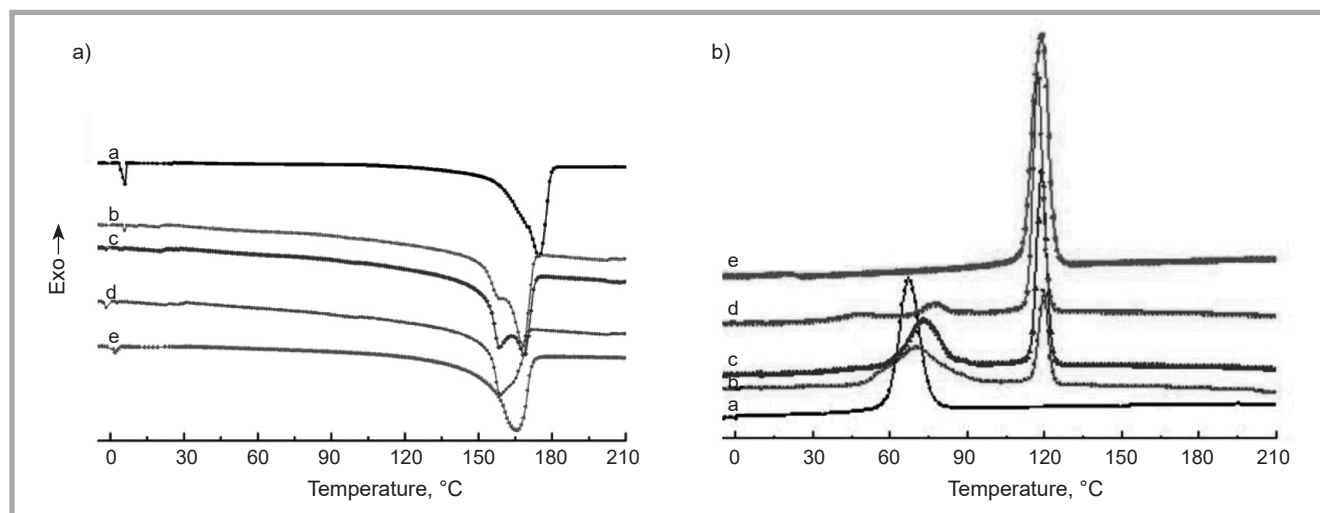


Figure 3. a) DSC thermograms of PHBV/PP-g-MAH blends from heating scans, b) DSC curves for PHBV/PP-g-MAH blends.

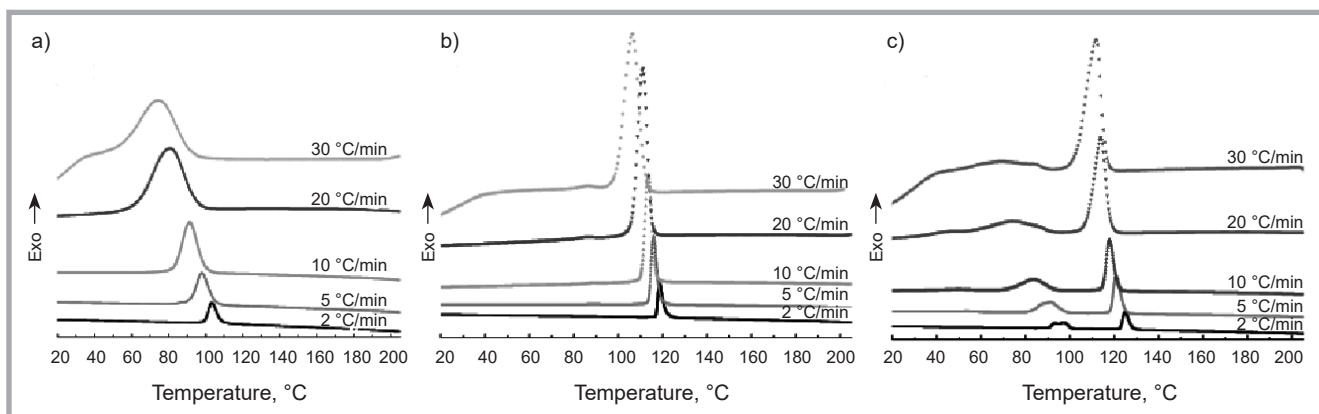


Figure 4. a) Nonisothermal crystallization DSC curves for PHBV at different cooling rates; b) Nonisothermal crystallization DSC curves for PP-g-MAH at different cooling rates, c) Nonisothermal crystallization DSC curves for PHBV/PP-g-MAH at different cooling rates.

DSC analysis

Figure 3.a and **3.b** show DSC thermograms of PHBV, PP-g-MAH and blends with different ratios in the cooling scan and second heating scan. The results are summarised in **Table 1**. It is observed that PHBV exhibits a crystallisation peak (T_c) at around 68.7 °C, an endothermic melting point (T_m) at 172.3 °C and a degree of crystallinity (X_c) of 50.4%. Neat PP-g-MAH shows T_c at around 120.1 °C and T_m of 168.2 °C. Two distinct glass transitions are observed for PHBV (at around 3.5 °C) and PP-g-MAH (at around -1.5 °C), attesting to the immiscibility of the two components in the blends, which is consistent with the result of SEM. However, as the mass ratio of PP-g-MAH increases in the blending system, T_g and T_m of PHBV and PP-g-MAH decrease, and the miscibility of PHBV/PP-g-MAH blending changes slightly in the amorphous region. In practice, the glass transition is a measure of the chain mobility in the amorphous phase; therefore it is critical in determining parameters for the drawing, texturing and dyeing of fibres and fabrics.

The crystallisation and melting peaks of PHBV and PP-g-MAH appear distinctly in the blends' thermograms, since the two components are completely immiscible. Both neat PHBV and PHBV/PP-g-MAH

blending have high crystallisation, but compared with PHBV, that of the blending system enhanced notably, which is consistent with literature [13, 15], which described that the crystallisation of the polymer with a lower T_g increased by blending the crystallisation of polymer with a higher T_g .

It can be seen from the DSC of the PHBV/PP-g-MAH blend system in the cooling curve that the blending system exhibits two endothermic peaks, which is proof of two kinds of phase in the PHBV/PP-g-MAH system. The crystallisation peak of PP-g-MAH is narrow and sharp due to its fast crystallisation process and perfect crystal structure. With an increase in PP-g-MAH content, the crystallisation temperature of PHBV increases, because PP-g-MAH forms small dense spherulite in the process of cooling rapidly, and becomes the crystal nucleus of PHBV, which induces the initial crystallisation of PHBV under a high temperature.

Nonisothermal crystallisation properties

In order to study the influence of temperature on the crystallization behavior of PHBV/PP-g-MAH, PHBV/PP-g-MAH blends were investigated by DSC at a different cooling rate. **Figure 4.a, 4.b** and **4.c** present the results of nonisothermal

crystallisation experiments. With an increase in the cooling rate of neat PHBV, the crystallisation temperature of neat PP-g-MAH and PHBV/PP-g-MAH decrease, and the crystallization peaks become wide. Chain activity is stronger under high temperature conditions, which is good for molecular chain segments i.e. making an orderly arrangement. At a lower temperature, the quantity of molecular diffusion to the crystalline phase increases, and part of the molecular chain in the crystal cell does not reach a steady state. Therefore the formation of the crystal is not perfect, and with an increase in the cooling rate, it became worse.

The crystallisation temperature and crystallisation peak of PP-g-MAH undergo few changes in PHBV/PP-g-MAH blends. Therefore the crystallisation behavior of PP-g-MAH has no effect on the cooling rate of the blends.

In the blending system, the crystallization temperature of PHBV is higher than that discussed in literature [14, 21]. PP-g-MAH in the cooling process forms a small dense spherulite, taken as the crystal nucleus, and then PHBV starts crystallisation under high temperature.

Rheological properties

The shear rheology is crucial for determining proper processing parameters for

Table 1. Thermal parameters for PHBV/PP-g-MAH blends.

m (PHBV)/ m (PP-g-MAH)	$T_{g1}/^{\circ}\text{C}$	$T_{g2}/^{\circ}\text{C}$	$T_{m1}/^{\circ}\text{C}$	$T_{m2}/^{\circ}\text{C}$	$T_{c1}/^{\circ}\text{C}$	$T_{c2}/^{\circ}\text{C}$	$\Delta H_{m1}/\text{J}\cdot\text{g}^{-1}$	$\Delta H_{m2}/\text{J}\cdot\text{g}^{-1}$	$X_c(\text{PHBV})/\%$
100/0	5.2	–	172.3	–	68.7	–	73.9	–	50.4
75/25	4.2	–	171.2	163.2	70.1	118.9	58.4	33.6	62.8
50/50	3.5	-2.2	170.2	163.6	72.4	119.8	40.5	36.3	52.4
25/75	2.1	-1.7	165.2	164.8	75.6	119.5	24.3	50.7	51.2
0/100	–	1.8	–	168.2	–	120.1	–	54.5	–

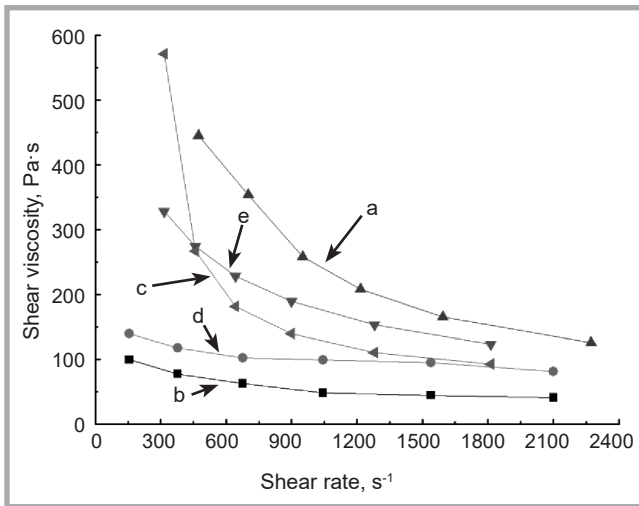


Figure 5. Flow curves for PHBV/PP-g-MAH blends.

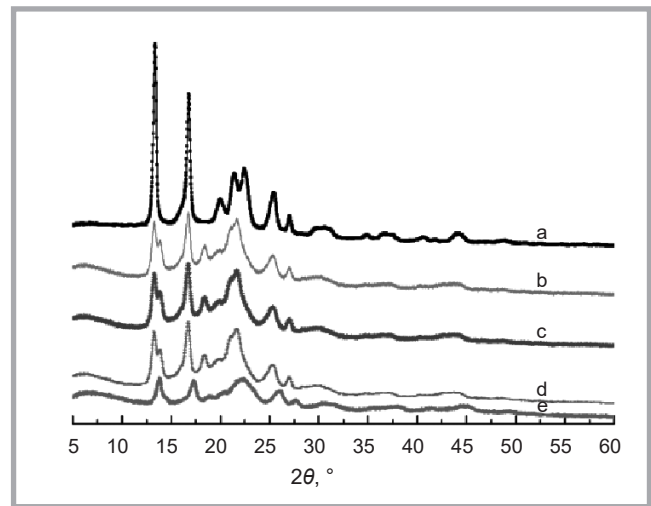


Figure 6. XRD patterns for PHBV/PP-g-MAH blends.

polymer products. Figure 5 shows the shear viscosity as a function of the shear rate at 190 °C for PHBV, PP-g-MAH and their blends. The shear viscosity of melting PHBV is higher than that of PP-g-MAH at the initial shear rate. For the blends, the viscosity decreases considerably as the PP-g-MAH content increases from 25% to 75% over the full shear rate range. Macromolecular chain activity is improved due to the interpenetration of the molecular chain of PHBV and PP-g-MAH in melting PHBV/PP-g-MAH blends. All the polymers show typical shear-thinning behavior, even at low shear rates, having the characteristics of pseudoplastic fluid. Shear stress increases with a higher shear rate, and macromolecular chain activity is enhanced, attributed to the removal of many nodes of the macromolecular chain. The shear viscosity of the melt decreases rapidly at a shear rate less than 500/s⁻¹, which shows that melting PHBV/PP-g-MAH blends is sensitive to change in the shear and nodes removal of the macromolecular chain in the blends.

Diffraction spectrum analysis

To better depict the crystallization of PHBV, PP-g-MAH and their blends, their XRD patterns are shown in Figure 6. These major diffraction peaks correspond to the (020), (110), (021), (101), (111), (121), (040) and (200) planes of PHBV, and the (110), (040), (130), (111) and (060) planes of PP-g-MAH, respectively [20, 22]. There is no (101) plane, corresponding to the diffraction peak at 2θ = 22.8°, in the PHBV/PP-g-MAH blends. The results show that the crystal form of PHBV/PP-g-MAH changes and two phases become compatible. As

PHBV or PP-g-MAH decrease at the same time, the diffraction peak intensity of the blends drops. It turns out that changing the proportion of blending prevents the formation of certain crystalline.

Spinning performance and morphology

Spinnability is evaluated by monitoring the fiber breakage frequency during 30 min spinning. Ranked by “+” in Table 2 (the more “+” appear, the better

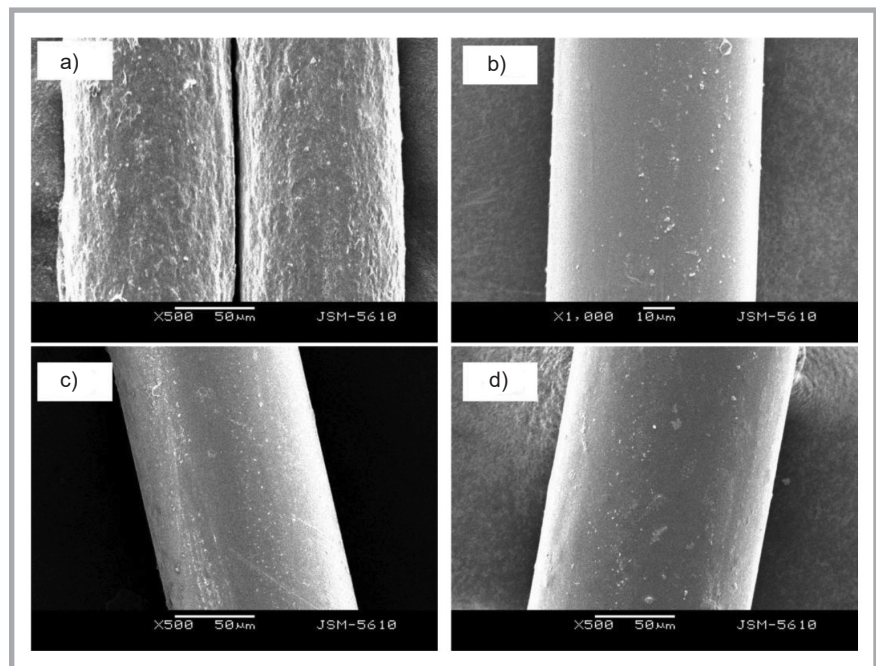


Figure 7. SEM images of PHBV/PP-g-MAH fibres, ratio of PHBV and PP-g-MAH: a) 75:25; b) 50:50; c) 25:75; (d) 0:100, 100% PHBV cannot be fabricated into fibre.

Table 2. Spinnability of PHBV and PHBV/PP-g-MAH at various take-up speeds. Note: The more “+” appear, the better the spinnability is.

Code	Spinnability at take-up speed, m/min			
	30	90	120	>300
A	–	–	–	–
b	+++	++	+	+
c	+++	+++	++	+
d	++++	++++	++++	+++
e	+++++	+++++	+++++	+++++

the spinnability is), the spinnability is positively affected by the PP-g-MAH addition. For instance, ϵ is ranked by “+++++” over the full speed range. As the PHBV content become higher than 75%, the fibers could not be wound at all at any speed studied. As a result, when the spinning speed reached 300 m/min, the spinning stickiness and breakage of PHBV were relatively improved with different amounts of PP-g-MAH added.

Figure 7 displays the surface morphology of PHBV/PP-g-MAH fibres. It is seen that the surface of PHBV/PP-g-MAH (75/25) fibre is rough, which may result from the exposure of PHBV on the fibre surface at room temperature and crystallization after rapid cooling. With the increasing amount of PP-g-MAH in the blend fibre, the surface roughness is gradually reduced. The surface smoothness of PHBV/PP-g-MAH (25/75) fibres is similar to that of pure PP-g-MAH fibre; also its evenness and fineness are increased.

Conclusions

On the whole PHBV and PP-g-MAH are two-phase incompatible according to the SEM of blends, while PHBV/PP-g-MAH blends represent different morphology with a change in PP-g-MAH addition. When PHBV and PP-g-MAH are at a mass ratio of 50:50, the distribution of PHBV/PP-g-MAH blends is the most compatible.

The initial thermal decomposition temperature of the PHBV/PP-g-MAH blends reaches over 250 °C, the thermal stability of PHBV is enhanced, and the processing window of PHBV is broadened by adding PP-g-MAH. Two distinct glass transitions are observed from DSC thermograms, attesting to the immiscibility of the two components in the blends. However, T_g and T_m of PHBV and PP-g-MAH decrease, and the miscibility of PHBV/PP-g-MAH blending shows a slight change in the amorphous region with an increase in the mass ratio of PP-g-MAH. With the growth of the cooling rate, the crystallization temperatures of neat PHBV, neat PP-g-MAH and PHBV/PP-g-MAH decrease, and the crystallization peaks of neat PP-g-MAH and PHBV/PP-g-MAH become wide.

PHBV/PP-g-MAH shows typical shear-thinning behavior even at low shear rates, having the characteristics of pseudoplastic fluid. PHBV/PP-g-MAH blends are sensitive to change in the shear.

The crystal form of PHBV/PP-g-MAH changes, the two phases become compatible, and the formation of certain crystal-line is prevented with a proper proportion of blending. When the spinning speed reaches 300 m/min, the spinning stickiness and the breakage of PHBV are relatively improved with different amounts of PP-g-MAH. added This can provide a theoretical basis for the preparation of PHBV/PP-g-MAH in the textile industry.

References

1. Reddy M, Vivekanandhan S, Misra M, Bhatia S, Mohanty A K. Biobased plastics and bionanocomposites: Current status and future opportunities. *Progress in Polymer Science* 2013; 38: 1653-1689.
2. Zhang Q, Liu Q, Mark JE, Noda I. A novel biodegradable nanocomposite based on poly (3-hydroxybutyrate-co-3-hydroxyhexanoate) and silylated kaolinite/silica core-shell nanoparticles. *Applied Clay Science*. 2009; 46: 51-56.
3. Kozłowska A, Gromadzki D, Fray M, Štěpánek P. Morphology Evaluation of Biodegradable Copolyesters Based on Dimerized Fatty Acid Studied by DSC, SAXS and WAXS. *FIBRES & TEXTILES in Eastern Europe* 2008; 16, 6(71): 85-88.
4. Mikołajczyk T, Król P, Boguń M, Krućńska I, Szparaga G, Rabej S. Biodegradable Fibrous Materials Based on Copolymers of Lactic Acid Obtained by Wet Spinning. *FIBRES & TEXTILES in Eastern Europe* 2013; 21, 3(99): 36-41.
5. Phukon P, Saikia JP, Konwar BK. Bio-plastic (P-3HB-co-3HV) from *Bacillus circulans* (MTCC 8167) and its biodegradation. *Colloids Surf. B Biointerf.* 2012; 92: 30-34.
6. Shan D, Zhang C, Kalaba S, Mehta N, Kim GB, Liu Z, Yang J. Flexible biodegradable citrate-based polymeric step-index optical fiber. *Biomaterials*. 2017; 143: 142-148.
7. Min Y, Lee S, Park J, Cho KY, Sung SJ. Effect of composition and synthetic route on the microstructure of biodegradable diblock copolymer, poly(ϵ -caprolactone-co-L-lactide) -b-poly(ethylene glycol). *Macromolecular Research*. 2008; 16 (3): 231-237.
8. Chen Y, Tan L, Chen L, Yang Y, Wang X. Study on biodegradable aromatic/aliphatic copolyesters. *Brazilian Journal of Chemical Engineering* 2008; 25(2): 321-335.
9. Majchrzycka M, Brochocka A, Grzybowski P. Modelling the Viability of Microorganisms of Poly(lactic Acid) Melt-Blown Nonwoven Fabrics for the Use of Respiratory Protection. *FIBRES & TEXTILES in Eastern Europe*. 2015; 23, 5(113): 107-113.
10. Zhu F, Han J, Yu B, Yu J, Ou L. Study on spinnability of biodegradable poly(3-hydroxybutyrate-co-3-hydroxyvalerate)/

- poly(lactic acid) blends for melt-blown nonwovens. *Journal of Textile Research*. 2016; 37(2): 19-24.
11. Zhu F, Yu B, Han J, Ding X. Spinnability of poly (lactic acid)/poly (3-hydroxybutyrate-co-3-hydroxyvalerate) for spun-bonded nonwovens. *Journal of Textile Research* 2014; 35(9): 21-26,
 12. Krikštanavičienė K, Stanys S, Jonaitienė V. Relation between Mathematically Simulated and Experimental Results of Polyhydroxybutyrate-co-valerate Yarns. *FIBRES & TEXTILES in Eastern Europe*. 2013; 21, 6(102): 27-32.
 13. Marcilla A, Garcia-Quesada J, Gil E. Behavior of flexible poly(vinyl chloride)/poly (hydroxybutyrate valerate) blends. *Journal of Applied Polymer Science* 2008; 110(4): 2102-2107.
 14. Gon Alves S, Martins-Franchetti S, Chinaglia D. Biodegradation of the Films of PP, PHBV and Its Blend in Soil. *Journal of Polymers and the Environment* 2009; 17(4): 280-285.
 15. Avella M, Martuscelli E, Raimo M. Review properties of blends and composites based on poly(3-hydroxy) butyrate (PHB) and poly(3-hydroxybutyrate-hydroxyvalerate)(PHBV) copolymers. *Journal of Materials Science* 2000; 35(3): 523-545.
 16. Sasikala C, Ramana C V. Biodegradable polyesters. *Advances in Applied Microbiology* 1996; (42): 97-218.
 17. Wojciechowska E, Fabia J, Ślusarczyk Cz, Gawłowski A, Wysocki M, Graczyk T. Processing and supermolecular structure of new iPP/PLA fibers. *FIBERS AND TEXTILES in Eastern Europe*, 2005; 13, 5(53): 126-128.
 18. Taguet A, Cassagnau P, Lopez-Cuesta J-M. Selective dispersion and compatibilizing effect of (nano)fillers in polymer blends. *Progress in Polymer Science* 2014; 39:1526-1563.
 19. Han H, Wang X, Wu D. Mechanical properties, morphology and crystallization kinetic studies of bio-based thermoplastic composites of poly(butylene succinate) with recycled carbon fiber. *Journal of Chemical Technology and Biotechnology* 2013; 88:1200-1211.
 20. Lei Y, Wu Q, Zhang Q. Morphology and properties of microfibrillar composites based on recycled poly (ethylene terephthalate) and high density polyethylene. *Composites Part A: Applied Science and Manufacturing* 2009; 40(6): 904-912.
 21. Lyon RE, Walters RN. Pyrolysis combustion flow calorimetry. *Journal of Mathematical Analysis and Applications* 2004; 71 :27-46.
 22. Buzarovska A, Grozdanov A. Crystallization kinetics of poly(hydroxybutyrate-co-hydroxyvalerate) and poly(dicyclohexylitaconate) PHBV/PDCHI blends: thermal properties and hydrolytic degradation. *Journal of Materials Science* 2009; 44: 1844-1850.

Received 20.07.2016 Reviewed 18.12.2017